Weierstraß-Institut
für Angewandte Analysis und Stochastik

im Forschungsverbund Berlin e.V.

Hysteresis in the context of hydrogen storage and lithium-ion batteries

Wolfgang Dreyer, Clemens Guhlke and Robert Huth

submitted: 26th February 2009

Weierstrass-Institute
for Applied Analysis
and Stochastics
Mohrenstr. 39
10117 Berlin
Germany
E-Mail: dreyer@wias-berlin.de
         guhlke@wias-berlin.de
         huth@wias-berlin.de

Abstract

The processes of reversible storage of hydrogen in a metal by loading and unloading and of charging and discharging of lithium-ion batteries have many things in common. Both processes are accompanied by a phase transition and loading and unloading run along different paths, so that hysteretic behaviour is observed.

For hydrogen storage we consider a fine powder of magnesium (Mg) particles and lithium storage is studied for iron phosphate ($FePO_4$) particles forming the cathode of a lithium-ion battery. The mathematical models that are established in [3] and [4], describe phase transitions and hysteresis exclusively in a single particle and on that basis they can predict the observed hysteretic plots with almost horizontal plateaus. Interestingly the models predict that the coexistence of a 2-phase system in an individual particle disappears, if its size is below a critical value. However, measurements reveal that this is qualitatively not reflected by the mentioned hysteretic plots of loading and unloading. In other words: The behaviour of a storage system consisting of many particles is qualitatively independent of the fact whether the individual particles itself develop a 2-phase system or if they remain in a single phase state.

This apparent paradoxical observation will be resolved in this article. It will be shown that if each of the individual particles homogeneously distributes the supplied matter, nevertheless the many particle ensemble exhibits phase transition and hysteresis, because one of the two phases is realised in some part of the particles while the remaining part is in the other phase.

1 Introduction and basic functionality of hydrogen storage and rechargeable lithium-ion batteries

Hydrogen is the ideal synthetic fuel to convert chemical energy into motive power, and currently rechargeable lithium-ion batteries are the most promising storage systems for electrical energy. The storage of hydrogen on interstitial lattice sites of certain metallic crystals and the principle of storage of lithium in the cathode of lithium-ion batteries have many things in common.

Both storage processes are accompanied by a phase transition and they exhibit hysteretic behaviour during loading and unloading, which is described in two characteristic diagrams: Hydrogen storage in metals is represented by the relation between the hydrogen vapor pressure of the device and the total amount of stored hydrogen,

and its counterpart in a lithium-ion battery is the relation between the voltage of the battery cell and its total charge. The voltage U is related to the difference of chemical potentials μ that will defined in a the later section:

$$U = -\frac{\mu}{e} + U_0, \tag{1}$$

where e denotes the charge of an electron and U_0 is the basic cell voltage.
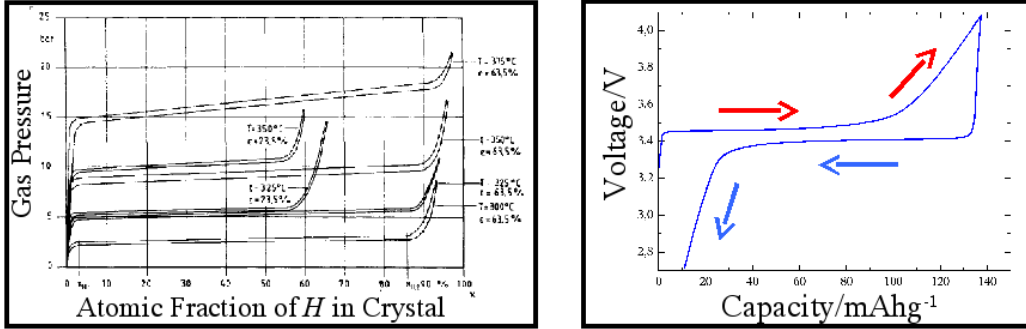

Figure 1: Left: Hydrogen vapor pressure versus hydrogen content per lattice site of Mg ([8]). Right: Voltage versus charge per mass of a $FePO_4$ cathode ([3])

In order to store hydrogen in a metal, e.g. magnesium (Mg), a hydrogen gas under some pressure is brought into contact with the metal offering interstitial lattice sites that can be occupied by hydrogen atoms. Similarly the cathode of lithium-ion batteries consists of a host system, e.g. the crystal iron phosphate ($FePO_4$), whose interstitial lattice sites likewise may serve to store lithium atoms. In the fully charged state of the battery, there is no lithium in the host system and it contains the maximal possible number of lithium atoms when the battery is fully discharged. Typical arrangements for simplified modelling are displayed in Figure 2. The device for hydrogen storage runs under fixed total volume and it contains a Mg particle and a certain amount of hydrogen gas. The process is as follows. For a temperature which depend on the storage substance, the H_2 gas molecules dissociates at the particle surface into atomic hydrogen, i.e. $H_2 - 2H = 0$, which hereafter enters the metal and occupies interstitial lattice sites. Depending on the total amount of hydrogen in the metal, a 2-phase system may develop. For small hydrogen content we have a solid solution, α-phase, and the relation between the gas pressure and the hydrogen content is approximately given by *Sievert law*, see [6, 15]. If the gas pressure exceeds a certain value, the formation of the hydride phase, β-phase, sets in. Further increase of the hydrogen content is now accompanied by coexistence of the two phases. In the coexistence region, the gas pressure remains constant at the van't Hoff pressure if the Mg particle can freely expand its volume. The volume changes because the hydrogen atom needs more space as is available by the interstitial lattice sites. If the extension of the particle is hindered, for example by the other particles, the slope of the coexistence pressure also will slightly change, which is displayed in Figure 1_{left}.
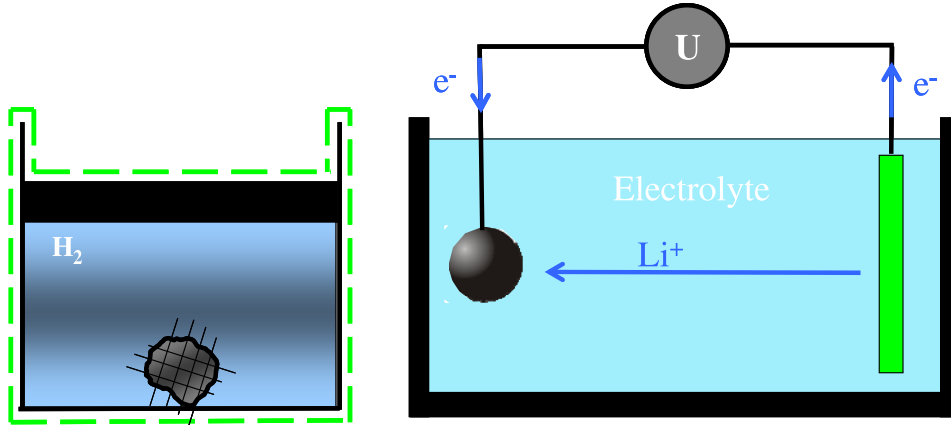
2

Figure 2: Left: A pressure vessel containing a Mg particle in contact to a hydrogen gas. Right: A $FePO_4$ particle against an metallic Li anode within an electrolyte.

Next we refer to Figure 2_{right} to explain the corresponding phenomena in lithium-ion batteries. The simplified device indicates the processes in a lithium battery during discharging and charging. During discharging electrons leave the anode, which consists here of metallic lithium, to travel through an outer circuit. The remaining positive lithium ions leave the anode and move through an electrolyte towards the cathode, which is the central object of the current modelling. It consists of a carbon coated single crystal $FePO_4$ with the shape of a small sphere of about 50 nm diameter. The $FePO_4$ lattice offers interstitial lattice sites that serve to store lithium atoms. When the battery is fully charged, all interstitial lattice sites are empty. During discharging the arriving lithium ions combine at the carbon coated surface of the $FePO_4$ ball with the inflowing electrons and hereafter they occupy the interstitial lattice sites. After complete discharging a maximal number of sites of the interstitial lattice is occupied by a lithium atom. During charging of the battery the reverse process takes place.

For small lithium content of the storage particle, the lithium atoms form a single phase that we likewise call α -phase. However, if the lithium content exceeds a certain value, the formation of a second phase, β-phase, sets in. Further increase of the hydrogen content is now accompanied by coexistence of the two phases. In the coexistence region, the gas pressure remains constant at the van't Hoff pressure if the Mg particle can freely expand its volume. The volume changes because the hydrogen atom needs more space as is available by the interstitial lattice sites. If the extension of the particle is hindered, for example by the other particles, the coexistence pressure will also slightly change. This is displayed in Figure 1_{left}.

Both host systems are not crystals of macroscopic size, rather they consist of fine powders of small $FePO_4$ respectively Mg particles. The decrease of particle size leads to an increase of the effective store capacity, namely the number of stored particles per available lattice sites. During the storage process there is a tremendous change of the particle volume, because the hydrogen atoms as well as the lithium atoms

need more space as is available by the lattice sites. For example the crystals may change their volume up to 30% in the hydrogen case and up to 6% during lithium storage. In particular for the hydrogen case, large particle would disintegrate into smaller ones.

The mathematical models, that were proposed in [3] and [4], describe phase transitions and hysteresis exclusively in a single particle and on that basis they can describe the observed hysteretic plots with almost horizontal plateaus. In particular the horizontal plateaus rely intimately on the occurrence of a 2-phase system with regions of high and small concentrations of the stored matter. Surprisingly there is the following phenomenon. When the size of an individual particle becomes too small the phase transition vanishes and the particle remains in a single phase state. This fact is observed in experiments, see [19], and additionally it results from the model equations. However, measurements reveal that this is not reflected by the mentioned hysteretic plots of loading and unloading. In other words: The behaviour of a storage system consisting of many particles is qualitatively independent of the fact whether the individual particles itself develop a 2-phase system or if they remain single phase.

In their paper on rate independent hysteresis from 2001, Truskinovski and Puglisi studied a closely related subject with the objective to explain hysteretic phenomena in shape memory alloys on a microscopic basis, [16]. The microscopic model consists of a one-dimensional chain of N oscillators with a non-monotone stress-strain characteristic that intimately corresponds to the non-monotone chemical potential-mole fraction characteristic, which play the essential role in this study. Differences of the two studies are the prescribed side conditions during the cycling of the hysteresis loop and the mathematical treatment.

The same subject is currently under investigation by Mielke and Truskinovski, [12]. In order to reduce the necessary assumptions that are needed in a quasi-static treatment of the problem, the authors rely the new reasoning of the behaviour of the chain model on an evolution law, and in addition to the non-monotone stress-strain characteristic they provide the oscillators with viscous elements and stochastic behaviour.

The analysis of a many particle system, where each particle is equipped with unstable states between two stable states, has been started already in 1982 by Dreyer, Müller and Strehlow, [5], where the equilibria of two connected spherical rubber balloons were seriously studied. That problem was generalized to $N > 2$ connected balloons by Kitsche, [9] in his diploma thesis, and the results, which form a complete analogy to the current problem and to Truskinovski and Puglisi, were published in [10] in 1987, see also chapter 5 for some more details of the analogy.

The paper is organized as follows: In chapter 2 we introduce the basic properties of the storage particles for hydrogen and lithium storage in juxtaposition. Chapter 3 introduces differences and similarities of both the storage problem from a thermodynamic viewpoint. Chapter 4 is addressed to the detailed exploitation of a simplified version of the slightly different models for hydrogen and lithium storage, so that

they both can be treated by the same non-monotone chemical potential function. Here we numerically illustrate the various phenomena and carry out mathematical analysis. Finally we have added a small Chapter 5, where we explain the intimate analogy between the many particle storage problems and the problem of the inflation of many connected rubber balloons via the supply of air.

2 Crystal structure and basic state variables of the host systems

In this chapter we describe the different crystal structures of the $FePO_4$ and the Mg particles, respectively. However, for the purposes of the current study we have slightly simplified the description, and we refer to the given citations for the complete and more precise details.

2.1 Crystal structure of $FePO_4$ for lithium storage

The configuration of an $FePO_4$ particle is illustrated in Figure 3. The $FePO_4$ units are indicated by yellow (Fe), pink (P), red (O) and the green balls are the interstitial lattice sites that can be occupied by the lithium atoms. The undeformed and
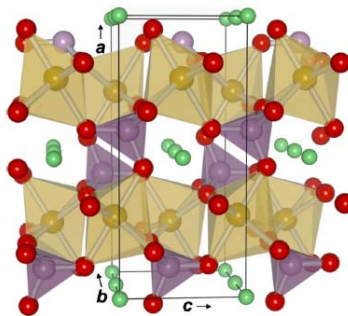

Figure 3: $FePO_4$ structure. Yellow: Fe, pink: P, red: O, green: interstitial sites. From [11]

deformed configuration of the host system is described in detail by T. Maxisch and G. Ceder in [11]. The undeformed crystal, which is the state where the sublattice formed by the interstitial lattice sites is completely empty, has orthorhombic olivine symmetry. To each unit of $FePO_4$ there corresponds one single site in the sublattice. In contrast to the behaviour of the Mg crystal, see below, the olivine structure does not change during the occupation of the sublattice sites by lithium atoms. If these are supplied or removed through the external boundary, there is a deformation of the olivine structure, because the lithium atoms need more space as it is available by the sublattice sites. Thus the crystal volume change if the number of Li atoms is

changed. Moreover the stiffness coefficients change. However, the crystal symmetry remains the same.

At room temperature there may exist a region of total Li concentration where the distribution of Li atoms on the sublattice sites is realised by two coexisting phases that differ by high and small Li concentrations. Theoretical studies on the evolution of Li atoms in the host system by Han et.al [7], Srinivasan and Newman [17] and the current study rely on this phenomenon, which is experimentally investigated by Yamada et.al. [20]. The crucial phenomenon that is addressed in this study is pointed out by Wagemaker et.al., [19]: The 2-phase region disappears if the particle size is below a critical value. In this case we have a pure solid solution which, however, is desirable because the power density of the battery should then be improved.

2.2   Basic state variables for lithium storage

The number N_{M} of $FePO_4$ units, which form the matrix lattice, is fixed. Thus we assume that there is no diffusion in the matrix lattice but it is deformed, and for simplicity we only take the change of its volume V_{P} into account and ignore deviatoric stresses, see [3] concerning the complete mechanical description.

On the sublattice of a particle we have N_{Li} Li atoms and N_{V} vacancies. The latter indicate the empty lattice sites, which do not have mass or momentum but they are carrier of energy and entropy. Because there is a single sublattice site to each $FePO_4$ unit, we have the side condition

$$N_{\mathrm{M}} = N_{\mathrm{Li}} + N_{\mathrm{V}}. \tag{2}$$

Thus for given temperature T, the basic variables of the lithium storage problem are V_{P}, N_{M} and N_{Li}. For the local description we introduce densities instead of numbers and to this end we introduce the mole densities n_{M}, n_{Li} and n_{V} which have units mole/m^3. Note that n_{M} changes because the volume V_{P} may change, whereas N_{M} is constant.

2.3   Crystal structure of Mg for hydrogen storage

The host system Mg for hydrogen storage exhibits more complexity as we have met in the lithium case. The natural Mg crystal at room temperature and atmospheric pressure has hexagonal-close-packed structure (hcp). Under pressure at about 50 GPa there is a martensitic phase transition to body-centered-cubic symmetry (bcc). By special quenching techniques into the temperature-pressure region of the storage process the bcc symmetry may survive and hereafter the storage system consists as a powder of small bcc Mg particles with diameters in the μm range. The interstitial lattice of a single Mg particle that is formed by the octahedral sites may be used now to store the hydrogen atoms. For each Mg atom there are 3 octahedral sites.

The storage process is as follows: At the surfaces of a single particle with volume V_P the molecules H_2 of the hydrogen gas dissociates into atomic hydrogen, which then may enter the Mg particles and occupy the described interstitial sites. The necessary temperature for dissociation is about $300\,°C$. Note that the dissociation temperature can be reduced by catalysts, but we do not consider this fact here.

For small hydrogen content we have a solid solution in the particles and that state is called the α-phase. Similar to lithium storage, the formation of the α-phase is accompanied by a change of the particle volume because an occupied site needs more space than an empty site. However, the bcc structure remains. There is a critical gas pressure, where the maximal solubility of hydrogen in the particles is reached. A so-called β-phase nucleates. The bcc structure transforms into tetragonal symmetry with rutile structure because MgH_2 is formed as it is indicated in Figure 4. There
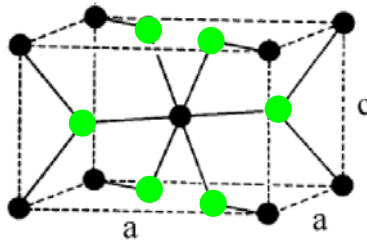

Figure 4: Rutile structure of MgH_2. Black: Mg, red: H. From [6]

is a region of total hydrogen content where α- and β-phase coexist and here the gas pressure remains almost constant, see Figure 1_{left}. The slight increase of the pressure is due to the fact that the Mg particles cannot freely expand their volume because they are slightly fixed by the other particles of the storage powder.

In the rutile structure of the β-phase we can identify further interstitial sites. After the whole crystal is in the β-phase, those sites also can be occupied by the hydrogen atoms for increasing gas pressure, as it is observed in Figure 1_{left}.

2.4 Basic state variables for hydrogen storage

The number N_M of Mg atoms, which form the matrix lattice, is fixed. Thus we assume that there is no diffusion in the matrix lattice but it is deformed, and for simplicity we only take the change of its volume into account and ignore deviatoric stresses, so that similarly to the lithium case, the stress tensor reduces to the pressure.

On the bcc sublattice of the α-phase we have N_H^α H atoms and N_V^α vacancies. There are $\eta_\alpha = 3$ sites to each Mg atom, thus here we have the side condition

$$\eta_\alpha N_M^\alpha = N_H^\alpha + N_V^\alpha. \tag{3}$$

Again for given temperature T, the basic variables of the α-phase are V_P, N_M^α and N_H^α. For the local description we introduce densities instead of numbers, namely the mole densities n_M, n_M^α, n_Li^α and n_V^α. Note that n_M changes because the volume may change, whereas N_M is constant.

On the rutile sublattice of the β-phase we have N_H^β H atoms and N_V^β vacancies. There are $\eta_\beta = 2$ sites to each Mg atom on the rutile sublattice, thus here we have the side condition

$$\eta_\beta N_\mathrm{M}^\beta = N_{\mathrm{H}_\eta}^\beta + N_{\mathrm{V}_\eta}^\beta. \tag{4}$$

The further sublattice of the β-phase has $\zeta_\beta = 3$ sites to each Mg atom of the rutile structure implying the side condition

$$\zeta_\beta N_\mathrm{M}^\beta = N_{\mathrm{H}_\zeta}^\beta + N_{\mathrm{V}_\zeta}^\beta. \tag{5}$$

Here the basic variables of the β-phase are V_P, N_M^β, $N_{\mathrm{H}_\eta}^\beta$ and $N_{\mathrm{H}_\zeta}^\beta$. The corresponding mole densities are n_M^β, $n_{\mathrm{H}_\eta}^\beta$, $n_{\mathrm{H}_\zeta}^\beta$, $n_{\mathrm{V}_\eta}^\beta$ and $n_{\mathrm{V}_\zeta}^\beta$.

3 Generic description of the different host systems

In this chapter we unify the description of the two different host systems. We begin with a short introduction into those basic facts of thermodynamics that are needed in the following.

3.1 A modicum of thermodynamics for a single storage particle

Global inequality. For lithium storage we consider a single $FePO_4$ particle without the surrounding and a single Mg particle which is immersed in a hydrogen gas for hydrogen storage, see Figure 2. For constant temperature and fixed pressure or fixed volume the 1th and 2nd law of thermodynamics states the temporal inequality

$$\frac{dA}{dt} \leq 0 \quad \text{with} \quad A = \Psi + p_0 V. \tag{6}$$

The quantity A is the available free energy of the system Ω at hand. Here A is the (Helmholtz) free energy plus outer pressure p_0 times the total volume of the system. In the lithium case $V = V_\mathrm{P}$, and for hydrogen storage we have $V = V_\mathrm{P} + V_\mathrm{G}$, where $V_\mathrm{P}, V_\mathrm{G}$ denote the particle and the gas volume, respectively.

In equilibrium the equality sign holds, whereas the available free energy must exclusively decrease in non-equilibrium. Thus the possible equilibria are determined by the minima of A.

There is a reason that we consider the electrolyte with volume V_E as an external medium, whereas the hydrogen gas is assumed to belong to the system Ω. The hydrogen gas exchanges hydrogen atoms with the storage particle and thus belongs to

the system. On the other hand, the electrolyte merely serves as an elastic medium that may produce a pressure on the $FePO_4$ particle. The lithium flux through its surface is not related to the electrolyte, rather it is given as an external flux whose rate is assumed to be small with respect to the temporal evolution of the internal phenomena, so that the available free energy of the $FePO_4$ particle approaches equilibrium at fixed total lithium content.

The role of the coexistence region of phases and of interfacial free energy. The free energy Ψ of the system under consideration consists of the sum of bulk free energies of the phases and of interfacial free energy that takes care for the interface between two adjacent phases. In [3] that contribution was related to the curvature of the α-β interfaces and it was shown that the surface tension may induce the hysteretic phenomenon. However, for the case of lithium storage the 2-phase coexistence region disappears for sufficiently small particles and this is illustrated in Figure 5, which shows that the sharp interface disappears for decreasing outer radius of the storage particle. This phenomenon is also described by Wagemaker et.al. in
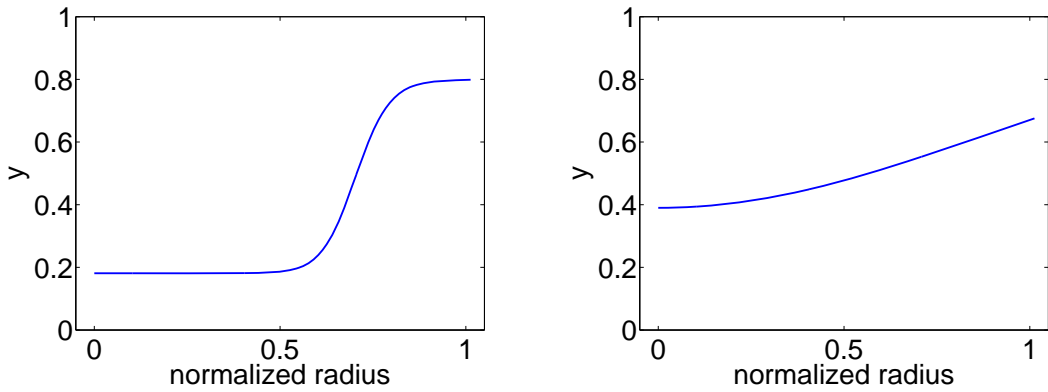

Figure 5: Interface region for outer radius r_0=20nm (left) and r_0=3nm (right). Calculation of the model from [3]

[19] and addionally the authors mention the observation of a similar behaviour in the case of hydrogen storage.

The main objective of the current study is the description of that case where a 2-phase region is energetically unfavorable for small particles. For this reason we assume that there are no interfaces. The individual storage particle is either in the α-phase or in the β-phase.

Free energy density, chemical potentials, pressure, Gibbs equation and Gibbs-Duhem equation. In the lithium case the free energy density $\rho\psi$ is defined so that

$$\Psi = \int_{\Omega_P} \rho_P \psi_P \, dx. \tag{7}$$

Here ρ_P is the mass density and ψ_P denotes the specific free energy in the particle. We have $\rho_P = m_M n_M + m_{Li} n_{Li} = n_M(m_M + m_{Li}y)$, where m_M and m_{Li} are the

molecular masses of $FePO_4$ and Li, respectively, and $y = n_{Li}/n_M$ gives the mole fraction of Li. These definitions hold for the α- as well as for the β-phase.

In the hydrogen case there in addition to the particle the hydrogen gas, and here Ψ is given by

$$\Psi = \int_{\Omega_P} \rho_P \psi_P dx + \int_{\Omega_{H_2}} \rho_{H_2} \psi_{H_2} dx. \tag{8}$$

$\rho_{H_2} = m_{H_2} n_{H_2}$ is the mass density of the gas. In the particle we have in the α-phase $\rho_P^\alpha = n_M^\alpha (m_M + m_H \eta y^\alpha)$, where $y^\alpha = n_H^\alpha/(\eta n_M^\alpha)$ denotes the hydrogen mole fraction of the α-phase. The corresponding expression in the β-phase reads $\rho_P^\beta = n_M^\beta(m_M + m_H * (\eta_\beta + \zeta_\beta) y^\beta)$, where $y^\beta = n_H^\beta/((\eta_\beta + \zeta_\beta) n_M^\beta)$. The total hydrogen mole fraction y^β of the β-phase can be related to the mole fractions of the two sublattices by $y^\beta = \eta_\beta/(\eta_\beta+\zeta_\beta) y_\eta^\beta + \zeta_\beta/(\eta_\beta+\zeta_\beta) y_\zeta^\beta$, with the sublattice mole fractions $y_\eta^\beta = n_{H_\eta}^\beta/(\eta_\beta n_M^\beta)$ and $y_\zeta^\beta = n_{H_\zeta}^\beta/(\zeta_\beta n_M^\beta)$.

Next we formulate the constitutive functions for the various specific free energies. For the lithium case the constitutive functions for the two phases have the same general form, namely

$$\psi^{\alpha,\beta} = \psi^{\alpha,\beta}(T, n_{Li}, n_V) = \tilde{\psi}^{\alpha,\beta}(T, y, n_M). \tag{9}$$

The representation via the function $\tilde{\psi}$ simply results from a transformation of the variables.

Similarly we write for the α-phase of the hydrogen case

$$\psi^\alpha = \psi^\alpha(T, n_H, n_V) = \tilde{\psi}^\alpha(T, y, n_M), \tag{10}$$

whereas for the β-phase with 2 sublattices we have more variables and the corresponding functions read

$$\psi^\beta = \psi^\beta(T, n_{H_\eta}, n_{H_\zeta}, n_{V_\eta}, n_{H_\zeta}) = \tilde{\psi}^\beta(T, y_\eta, y_\zeta, n_M). \tag{11}$$

Finally we give the constitutive function for the hydrogen gas, which is a single substance, so that we simply may write

$$\psi^{H_2} = \psi^{H_2}(T, n_{H_2}) \tag{12}$$

The generic form of the functions $\psi(T, n_1, n_2, ..., n_\nu)$ satisfies the Gibbs equation and the Gibbs-Duhem equations, see [2] and [13]. These read

$$d\rho\psi = -\rho s dT + \sum_{a=1}^{\nu} \mu_a dn_a \quad \text{and} \quad p = -\rho\psi + \sum_{a=1}^{\nu} \mu_a n_a, \tag{13}$$

where the newly introduced quantities are the chemical potentials μ_a and the pressure p. We conclude from $(12)_1$ and by an easy calculation

$$\mu_a = \frac{\partial \rho\psi}{\partial n_a} \quad \text{and} \quad p = -\rho\tilde{\psi} + n_M \frac{\partial \rho\tilde{\psi}}{\partial n_M} = -\rho n_M \frac{\partial \tilde{\psi}}{\partial n_M}. \tag{14}$$

10

The representations (14) give the central quantities of the current study.

Necessary conditions for equilibria. The available free energy A depends on the participating volumes and on the various sets of mole densities that are described above. In order to obtain the necessary conditions for the possible equilibria the first derivatives of the available free energy with respect to the corresponding variables must be set equal to zero. The resulting conditions can be assigned to 3 kinds of equilibria, namely mechanical equilibria, chemical equilibria and phase equilibria. Recall that we consider in this study exclusively the case that a single particle is either in α- or in β-phase, so that conditions for interfacial phase equilibrium do not occur here.

In the case of lithium storage we have thus only mechanical equilibrium, which reads

$$p_{\mathrm{P}}^{\alpha,\beta} = p_{\mathrm{E}} \quad \text{and} \quad p_{\mathrm{E}} = p_0, \tag{15}$$

where p_{E} is the pressure on the particle surface that is induced by the electrolyte.

Note, if we were to consider a 2-phase system in a single particle, then interfacial phase equilibrium were characterized by $\mu_{\mathrm{Li}}^{\alpha} = \mu_{\mathrm{Li}}^{\beta}$ and $\mu_{\mathrm{V}}^{\alpha} = \mu_{\mathrm{V}}^{\beta}$.

For hydrogen storage the conditions for mechanical equilibrium are

$$p_{\mathrm{P}}^{\alpha,\beta} = p_{\mathrm{H}_2} \quad \text{and} \quad p_{\mathrm{H}_2} = p_0. \tag{16}$$

In this case we also have phase equilibrium, namely between the particle and the hydrogen gas. This gives rise to the conditions

$$\mu_{\mathrm{H}}^{\alpha} - \mu_{\mathrm{V}}^{\alpha} = \frac{1}{2}\mu_{\mathrm{H}_2} \quad \text{and} \quad \mu_{\mathrm{H}_{\eta_\beta}}^{\beta} - \mu_{\mathrm{V}_{\eta_\beta}}^{\beta} = \frac{1}{2}\mu_{\mathrm{H}_2} \tag{17}$$

Because the β-phase consists of 2 sublattices, there is also a condition for chemical equilibrium, which describes the transition of hydrogen atoms and vacancies between the sublattices. That condition reads

$$\mu_{\mathrm{H}_{\eta_\beta}}^{\beta} - \mu_{\mathrm{V}_{\eta_\beta}}^{\beta} = \mu_{\mathrm{H}_{\zeta_\beta}}^{\beta} - \mu_{\mathrm{V}_{\zeta_\beta}}^{\beta}. \tag{18}$$

The explicit evaluation of the necessary conditions for equilibrium require constitutive equations for the specific free energies. Afterwards we shall give those equations for a simplified version of the model.

Assumption on the approach of the storage systems to the various equilibria. The approach of the storage systems to mechanical equilibrium is the fastest process, and for this reason we assume that the system is at any time in mechanical equilibrium. This assumption allows to eliminate the mole densities of the matrix lattice from the list of variables. The same assumption is made here concerning chemical equilibrium of the β-phase in the case of hydrogen storage, implying that by means of (18) with (18) and assumed invertibility we also may eliminate $y_{\zeta_\beta}^{\beta}$, so that we now may use the total mole fraction y^{β} as the only hydrogen mole fraction of the β-phase. For both storage problems and for all phases we thus end up with specific free energies that depend exclusively of the lithium, respectively the total hydrogen mole fraction.

3.2 The available free energies of many particle systems

Now we consider the many particle problem as it is indicated in Figure 6. We have N particles, indexed by $l \in 1, 2, ..., N$, in the considered system, and we assume that each of the particles are either in α- or in β-phase and their state variables are homogeneous.
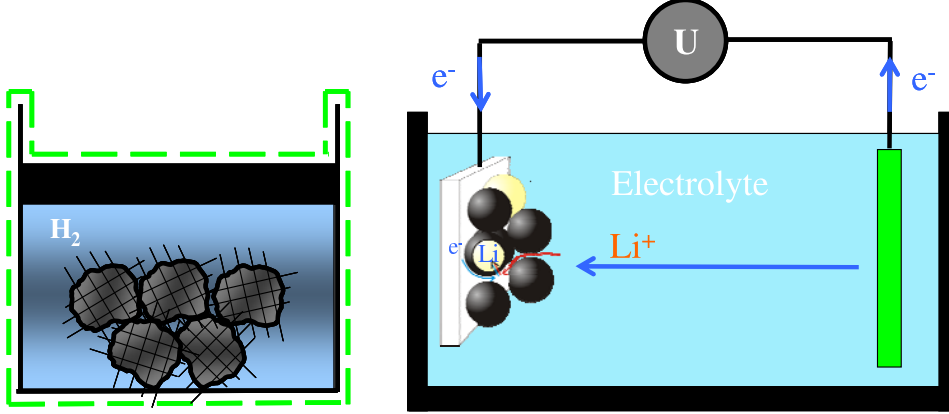

Figure 6: Left: A pressure vessel containing a powder of many Mg particles in contact to a hydrogen gas. Right: A cathode coated with many $FePO_4$ particles against an metallic Li anode within an electrolyte.

Lithium storage. Here the available free energy is given by

$$A = \sum_{l=1}^{N} \int_{\Omega_l} (\rho^l \psi^l + p_E) dx = \sum_{l=1}^{N} V^l (\rho^l \psi^l + p_E), \tag{19}$$

where V^l is the volume of particle l.

The behaviour of A is restricted to various side conditions that we formulate next. (i) The number N_M^l of matrix molecules ($FePO_4$) is constant and the same for each storage particle $N_M^l = N_M^1, l = 1, \cdots, N$. (ii) The empty particles have the same volume $\bar{V}$ and thus the same mole density $\bar{n}_M$. (iii) The total number of Li atoms, N_{Li}, in the many particle system is constant. Thus we have

$$N_M^l = n_M^l V^l = \bar{n}_M \bar{V}, \qquad\qquad N_{Li}^l = n_{Li}^l V^l, \tag{20}$$

$$N_M = \sum_{l=1}^{N} N_M^l = N \bar{n}_M \bar{V}, \qquad\qquad N_{Li} = \sum_{l=1}^{N} N_{Li}^l . \tag{21}$$

The macroscopic filling degree of all particles $q = N_{Li}/N_M$ denoting the overall loading state of the system is therefore constant and can then be written as

$$q = \frac{\sum_{l=1}^{N} N_{Li}^l}{N_M} = \frac{1}{N} \sum_{i=1}^{N} y_i . \tag{22}$$

Hydrogen storage. The system for hydrogen storage includes the N Mg particles and additionally the gas, so that its available free energy reads

$$A = \sum_{l=1}^{N} \int_{\Omega_l} \rho^l \psi^l dx + \int_{\Omega_{\mathrm{H}_2}} \rho_{H_2} \psi_{H_2} dx + p_0 V = \sum_{l=1}^{N} V^l \rho^l \psi^l + V_{\mathrm{G}} \rho_{H_2} \psi_{H_2} + p_0 V, \quad (23)$$

where $V = V_{\mathrm{P}} + V_{\mathrm{G}}$ is the total volume of the system.

Also in this case we consider various side conditions. (i) The number N_{M}^l of Mg atoms is constant and the same for each storage particle $N_{\mathrm{M}}^l = N_{\mathrm{M}}^1, l = 1, \cdots, N$. (ii) The empty particles have the same volume $\bar{V}_{\mathrm{P}}$ and thus the same mole density $\bar{n}_{\mathrm{M}}$. (iii) The total volume, $\bar{V}$ of the system is constant. (iv) The total number of H atoms, N_{H}, in the system is constant. Thus we have

$$N_{\mathrm{M}}^l = n_{\mathrm{M}}^l V^l = \bar{n}_{\mathrm{M}} \bar{V}_{\mathrm{P}}, \qquad\qquad N_{\mathrm{H}}^l = n_{\mathrm{H}}^l V^l, \qquad\qquad (24)$$

$$N_{\mathrm{M}} = \sum_{l=1}^{N} N_{\mathrm{M}}^l = N \bar{n}_{\mathrm{M}} \bar{V}, \qquad\qquad N_{\mathrm{H}} = 2 N_{\mathrm{H}_2} + \sum_{l=1}^{N} N_{\mathrm{H}}^l, \qquad\qquad (25)$$

$$n_{\mathrm{H}_2} = \frac{N_{\mathrm{M}}}{N} \left(\frac{Nq - \sum_{l=1}^{N} y^l}{V_{\mathrm{G}}} \right), \qquad\qquad V_{\mathrm{G}} = \bar{V} - \frac{N_{\mathrm{M}}}{N} \sum_{l=1}^{N} \frac{1}{n_{\mathrm{M}}^l}, \qquad\qquad (26)$$

where the macroscopic filling degree of the total system $q = N_{\mathrm{Li}}/N_{\mathrm{M}}$ is defined as the sum of the filling degree of all particles plus a part that takes care for the amount of hydrogen in the gas:

$$q = \frac{\sum_{l=1}^{N} N_{\mathrm{H}}^l}{N_{\mathrm{M}}} = \frac{1}{N} \sum_{l=1}^{N} y_l + \frac{V_{\mathrm{G}}}{N_{\mathrm{M}}} n_{\mathrm{H}_2} . \qquad\qquad (27)$$

3.3 Simplified version of explicit constitutive equations

Note that so far we did not quote any explicit constitutive equation for the various substances that are involved in the two storage problems. Relying on Section 3.1 it is obvious that the knowledge of the various specific free energies allows to calculate the constitutive laws for the pressures and the chemical potentials which are the crucial quantities that determine the evolution of the storage systems. The usual procedure, however, is different. It relies on the observation, that a free energy density can be additively decomposed into an chemical part, that exclusively depends on the mole fraction y, and a mechanical part that depends on the mole fractions and on the mole densities n_{M}. We write $\rho\psi = \rho\psi^{\mathrm{chem}} + \rho\psi^{\mathrm{mech}}$, and refer the reader to the careful discussion of these definitions in [2]. The reason for the decomposition of the free energy is due to the fact that we knowledge of ψ^{chem} and ψ^{mech} results from different sources. While ψ^{chem} is given directly either by measurements or by models within the setting of statistical mechanics, follows ψ^{mech} via 14_2 by integration from a constitutive law for the pressure.

Constitutive functions for the pressures. The storage particles are assumed to be elastic with misfit strain, which is due to the volume expansion during the loading by lithium respectively hydrogen atoms. The misfit strain is given by $h(y) = 1/(1+\delta y)$ with $\delta = (V_{\max} - V_R)/V_R$, and the generic constitutive law for the pressure p_P of a particle is assumed to be given by

$$p_P = p_R + K(y)(\frac{n_M}{n_M^R} - h(y)). \tag{28}$$

We have $\delta \approx 0.06$ and $\delta \approx 0.3$ for lithium storage, respectively hydrogen storage. p_R is the reference pressure and V_R denotes the reference volume, which is assumed by an empty storage particle, and $K(y)$ is the concentration dependent bulk modulus. However, that dependence will be ignored here.

The pressure of the electrolyte is similar formed. We write

$$p_E = p_R + K_E(\frac{V_E^0}{V_E} - 1), \tag{29}$$

where K_E is the bulk modulus of the electrolyte and V_E is its actual volume which is related to the reference volume V_E^0 according to $V_E = V_E^0(1 - \delta q)$. Recall that the filling degree is related to the mole fractions by 22.

Finally we give the pressure for the hydrogen gas that is assumed to be an ideal gas, so that we have

$$p_{H_2} = n_{H_2} RT, \tag{30}$$

with the universal gas constant $R = 8.31$ J/(mole K).

Mechanical parts of free energies. By integration of 14_2 we obtain the mechanical part of the free energy density of the particles. It reads

$$\rho\psi^{\mathrm{mech}} = (p_R - Kh(y))(\frac{n_M}{n_M^R h(y)} - 1) + K\frac{n_M}{n_M^R} \log \frac{n_M}{n_M^R h(y)}. \tag{31}$$

The corresponding free energy density for the electrolyte is not needed, because it does not belong to the considered system, and the mechanical part of the free energy density of the hydrogen gas results as

$$\rho_{H_2}\psi_{H_2}^{\mathrm{mech}} = RT \log \frac{p_{H_2}}{p_R}. \tag{32}$$

Chemical parts of free energies. In the case of lithium storage the chemical part of the free energy can be given by simple function for both phases, because the crystal structure is the same for low as well as high lithium content of a particle. We use here the same non-convex constitutive law as in [3] that takes entropic parts and the heat of solution into account. It reads

$$\rho\psi^{\mathrm{chem}} = n_M L f(y) \tag{33}$$

with

$$f(y) = a_1(T)y + a_2(T)(1-y) + y(1-y) + \frac{RT}{L}(y \log y + (1-y) \log(1-y)), \tag{34}$$

where $L > 0$ is the constant heat of solution. $a_1(T)$ and $a_2(T)$ are not important in this study because we consider here isothermal processes.

The case of hydrogen storage is more subtle, because as described above the crystal structure changes if the phases change, so that we different function are needed for different phases. These functions turn out to be both parabola, because the solid solution as well as the formation of hydride are exothermic and thus have negative heat of solutions, see the forthcoming article [4]. Here we simply interpolate between the both functions and take as the result the same structure as (33).

The chemical part of the free energy density of the hydrogen gas has only entropic contributions and because the gas is ideal and consists of a single substance, it is of the simple form

$$\rho_{H_2}\psi_{H_2}^{chem} = n_M a_3(T). \tag{35}$$

As before we do not specify here the temperature dependent function $a_3(T)$ and refer again to [4].

Chemical potentials. In order to calculate the chemical potentials we construct from the above at first the function $\psi(T, n_{Li,H}, n_V)$, $\psi_{H_2}(T, n_{H_2})$, and use then (14_1) to obtain for lithium, respectively hydrogen

$$\frac{1}{L}\mu_{Li,H} = f(y) + (1-y)f'(y) +$$
$$b_1\left(\log(\frac{n_M}{\bar{n}_M h}) - \frac{h'}{h}(1 - \frac{\bar{n}_M h}{n_M})(1-y)\right) + b_2\left(1 - \frac{h'}{h}(1-y)\right)\frac{1}{h}, \tag{36}$$

and for the vacancies

$$\frac{1}{L}\mu_V = f(y) - yf'(y) + b_1\left(\log(\frac{n_M}{\bar{n}_M h}) + \frac{h'}{h}(1 - \frac{\bar{n}_M h}{n_M})y\right) + b_2\left(1 + \frac{h'}{h}y\right)\frac{1}{h}. \tag{37}$$

The newly introduced constants $b_1 = K/n_M^R L$ and $b_2 = p_R/n_M^R L$ control the strength of mechanical in comparison to chemical contributions.

Finally chemical potential of the hydrogen gas results as

$$\mu_{H_2} = a_3 + RT\log\frac{p_{H_2}}{P_R}. \tag{38}$$

3.4   Exploitation of mechanical equilibrium

As it was explained in Section 3.1 the assumption that mechanical equilibrium is established at any time allows to determine the mole density n_M of the matrix by the mole fraction y, so that we end up with free energy densities and chemical potentials that depend exclusively on y.

Lithium storage. For each single phase FePO$_4$ particle with index $l \in 1, 2, .., N$ we have according to (15) and (28)

$$p(y^l, n_M^l) = p_E \quad \text{implying} \quad K(\frac{n_M^l}{\bar{n}_M} - h(y^l)) = K_E\delta q, \tag{39}$$

which gives the function $n_M^l = \hat{n}_M^l(y^l, q)$.

Hydrogen storage. For each single phase Mg particle with index $l \in 1, 2, .., N$ that is immersed in the gas we have according to (31) and (29)

$$p(y^l, n_M^l) = p_{H_2} \quad \text{implying} \quad p_R + K\left(\frac{n_M^l}{\bar{n}_M} - h(y^l)\right) = n_{H_2} RT. \tag{40}$$

The density of the g as molecules depend via (26) on the mole fraction, on the filling grade and(!) on all mole densities n_M^1, n_M^2, ..., n_M^N. However, an estimate shows that this dependence is quite small and thus can be ignored. The result is again a function of the type $n_M^l = \hat{n}_M^l(y^l)$.

4 The many particle system in detail

4.1 Determination of equilibria

Lithium storage. Under the assumptions (20) and (39) the available free energy (19) reduces to

$$A(y^1, \ldots, y^{N-1}) = \frac{N_M}{N} \sum_{\ell=1}^N \left(\frac{1}{\hat{n}_M^l} \rho^l \psi^l + \frac{p_E}{\hat{n}_M^l}\right) \quad \text{with} \quad y_M^N = Nq - \sum_{l=1}^{N-1} y^l . \tag{41}$$

Next, we define the difference of the chemical potential $\mu = \mu_{Li} - \mu_V$ this is related to the free energy of each particle by

$$\mu = \frac{1}{n_M} \frac{\partial \rho_P \psi_P}{\partial y} . \tag{42}$$

Note that the chemical potential depends on the mole density n_M and the mole fraction y. However, the mole density depends by the equation (39) only on the mole fraction y an we define $\hat{\mu}(y) = \mu(y, \hat{n}_M)$.

The free available energy has a minimum at any equilibrium point. The necessary conditions for equilibria are

$$0 = \frac{\partial A}{\partial y^l} = \frac{N_M}{N}\left(\hat{\mu}(y^l) - \hat{\mu}(y^N)\right) . \tag{43}$$

This means that the voltage of each particle is the same. The sufficient condition for equilibria can be read of the Hessian

$$\frac{\partial^2 A}{\partial y^l \partial y^k} = \frac{N_M}{N}\left(\frac{\partial \hat{\mu}}{\partial y}\bigg|_{y=y^l} \delta_{lk} + \frac{\partial \hat{\mu}}{\partial y}\bigg|_{y=y^N}\right) . \tag{44}$$

and will be evaluated in the next section.

Hydrogen storage. Under the assumptions (24) and (40) the available free energy (23) reduce to

$$A(y^1, \ldots, y^N) = \frac{N_{\mathrm{M}}}{N} \sum_{l=1}^{N} \frac{1}{\hat{n}_{\mathrm{M}}^l} \rho^l \psi^l + V_{\mathrm{H}_2} \rho_{\mathrm{H}_2} \psi_{\mathrm{H}_2} + \bar{V} p_0 \tag{45}$$

with

$$n_{\mathrm{H}_2} = \frac{N_{\mathrm{M}}}{N} \left(\frac{Nq - \sum_{\ell=1}^{N} y^\ell}{V_{\mathrm{H}_2}} \right) \quad \text{and} \quad V_{\mathrm{H}_2} = \bar{V} - \frac{N_{\mathrm{M}}}{N} \sum_{l=1}^{N} \frac{1}{\hat{n}_{\mathrm{M}}^l} \ . \tag{46}$$

Similar to the lithium case, we define the difference of the chemical potential $\mu = \mu_{\mathrm{H}} - \mu_{\mathrm{V}}$ this is related to the free energy of each particle by

$$\mu = \frac{1}{n_{\mathrm{M}}} \frac{\partial \rho_{\mathrm{P}} \psi_{\mathrm{P}}}{\partial y} \ . \tag{47}$$

Note that the chemical potential depends on the mole density n_{M} and the mole fraction y. However, the mole density depends by the equation (40) only on the mole fraction y an we define $\hat{\mu}(y) = \mu(y, \hat{n}_{\mathrm{M}})$.

The necessary conditions for equilibria are

$$0 = \frac{\partial A}{\partial y^l} = \frac{N_{\mathrm{M}}}{N} \left(\hat{\mu}(y^l) - \frac{1}{2} \mu_{\mathrm{H}_2}(n_{\mathrm{H}_2}) \right) \tag{48}$$

and the Hessian is

$$\frac{\partial^2 A}{\partial y^l \partial y^k} = \frac{N_{\mathrm{M}}}{N} \left(\frac{\partial \hat{\mu}}{\partial y} \Big|_{y=y^l} \delta_{lk} - \frac{1}{2} \frac{\partial \mu_{\mathrm{H}_2}}{\partial n_{\mathrm{H}_2}} \frac{\partial n_{\mathrm{H}_2}}{\partial y^k} \right) \ , \tag{49}$$

where

$$\frac{\partial n_{\mathrm{H}_2}}{\partial y^k} = -\frac{N_{\mathrm{M}}}{N V_{\mathrm{H}_2}} \left(1 + V_{\mathrm{M}}^k \frac{n_{\mathrm{H}_2}}{n_{\mathrm{M}}^k} \frac{\partial \hat{n}_{\mathrm{M}}}{\partial y^k} \right) \ . \tag{50}$$

General structure. A generic formulation for available free energy in both cases is

$$A(x) = \frac{1}{N} \left(\sum_{\ell=1}^{N_*} F(y_\ell) + F_2(q, x) \right) \tag{51}$$

Where $x \in \Lambda$ and $\Lambda = \mathbb{R}^{N_*}$ the space of possible system states. For the lithium model $N_* = N - 1$ and $F_2(q, x) = F(y_N)$ (confer (22)), whereas by (24) $N_* = N$ and F_2 is a convex function. The Hessian in this notation reads

$$D_x^2 A(x) = H(x) = \frac{1}{N} \left(\begin{pmatrix} F''(y_1) & & \\ & \ddots & \\ & & F''(y_{N-1}) \end{pmatrix} + D_x^2 F_2(q, x) \right) \ . \tag{52}$$
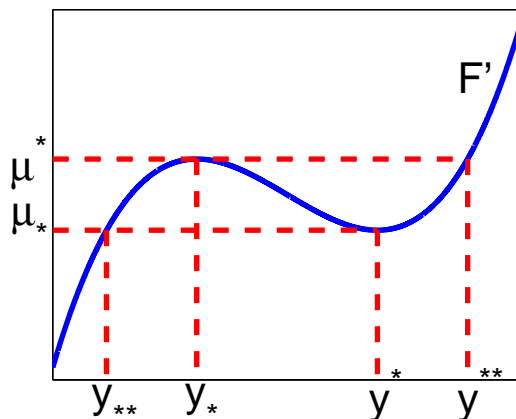
Figure 7: Qualitative description of particle potential

The crucial point in the following discussion, is that $F' \in C^1$ is a nonmonotone function. It is strictly decreasing in an interval (y_*, y^*) and strictly increasing else.

Note, that the Hessian is guaranteed to be positive definite if $F''(y_\ell) > 0$ for all ℓ. Another property which will be needed later is the fact, that the matrix $D_x^2 F_2(q, x)$ all entries in each row are the same. For the lithium model $F_2(q, x) = F(Nq - \sum_{\ell=1}^{N_*} y_\ell)$

Numerical exploitation. To evaluate the necessary conditions, we solve a system of nonlinear equations. Figure 8 shows possible solutions in the lithium case. The figure indicates that for an increasing number of particles the number of possible solutions increases for one filling degree q.

One observation is that if $\partial \hat{\mu} / \partial y$ is positive for all particles, then the Hessian of the system is always positive definite. For increasing numbers of particles, we observe that there is almost no equilibria for one particle in a state where $\partial \hat{\mu} / \partial y$ is negative.

This gives rise to the model assumption that no particle should ever be in the intermediate region. We can now formulate the following lemma.

Lemma 1 (There are almost no equilibria states possible with one particle in the intermediate region). *The lemma consists of two statements. For fixed q let the necessary equilibria condition be fulfilled, then we can say*

- (i) *if two or more particles are in the intermediate region, then the second derivative is Negative definite.*

- (ii) *if only the k-th particle is in the intermediate region, then its state y_k must be, depending on N, arbitrary close to the boundary of the intermediate region.*

Note, if $H(x)$ is negative definite for the system-state x, then x is not an energy minimum.
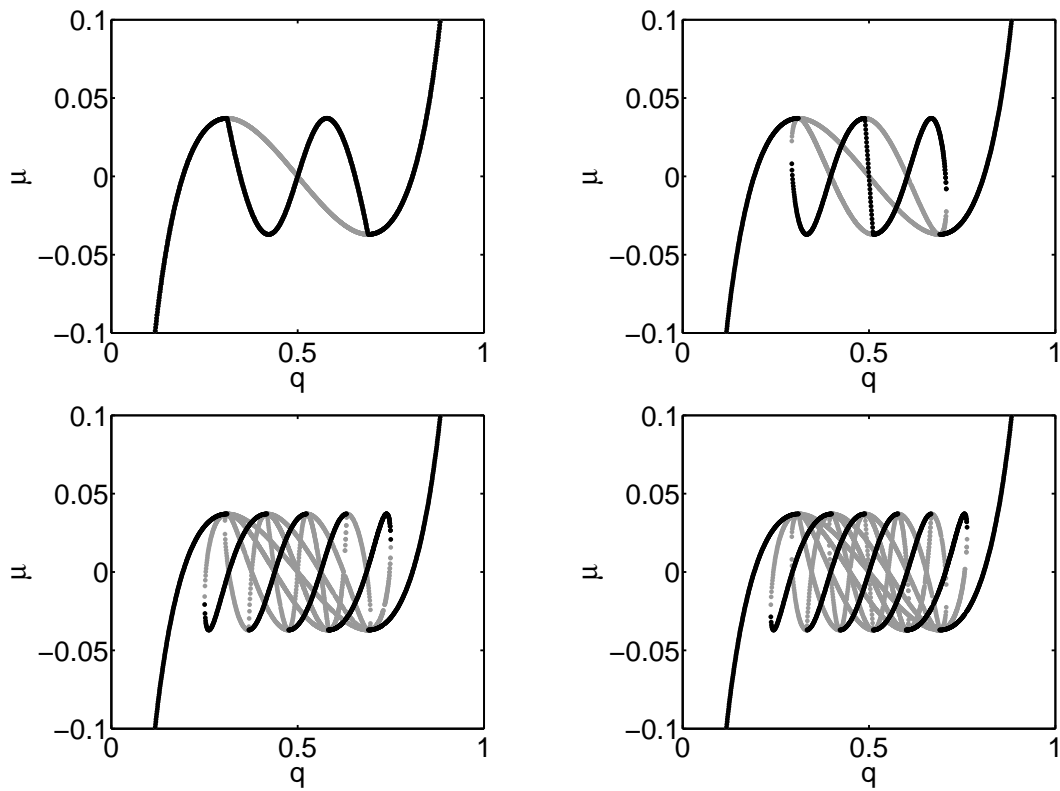
Figure 8: Solutions of the necessary conditions of 2,3,5 and 6-particle system, black indicates equilibria and grey indicates non-equilibria

Proof. We denote by e_k the k-th unitvector, which has an entry 1 at the k-th position and zero entries otherwise.

The lithium storage model

  (i) Let particles k and ℓ be in the intermediate region.
    $\Rightarrow F''(y_k), F''(y_\ell) < 0$
    (a) $k, \ell < N \Rightarrow x := e_k - e_\ell,$ $x^T [H(x)] x < 0$
    (b) $\ell < N, k = N \Rightarrow x := e_\ell,$ $x^T [H(x)] x < 0$

  (ii) Particle k is in the intermediate region.
    $\Rightarrow F''(y_k) < 0$
    (a) $k < N \Rightarrow x := e_k - \frac{1}{N_*} \sum_{i=1, i \neq k}^{N-1} e_i,$
    (b) $k = N \Rightarrow x := \frac{1}{N_*} \sum_{i=1}^{N-1} e_i,$
    Then in both cases there holds

$$N \ x^T [H(x)] x = F''(y_k) + \frac{1}{(N-1)^2} \sum_{i=1, i \neq k}^{N} F''(y_i) . \tag{53}$$

It turns out that

$$|F''(y_k)| < \frac{\frac{1}{N-1} \sum_{i=1, i \neq k}^{N} F''(y_i)}{N - 1} \tag{54}$$

must be true, if (53) should be positive. Since F'' is bounded this is equivalent to $F''(y_k)$ being arbitrarily close to zero. By assumption F'' is continuous and only zero at the boundary of the intermediate region, which proves the assertion.

The hydrogen storage Model The prove is exactly the same and the only extra ingredience is the special structure of $D_x^2 F_2$ in the hydrogen case. $\qquad\qquad\square$

4.2   Stable path

Recall that the available free energy $A(x, t)$ depends not only on the system state $x \in \Lambda$ but also on time. In our case the time dependence enters with the given continuous evolution of $q(t)$. Therefore the energy landscape changes in time. We consider the system to be quasi static. Therefore the dynamic behaviour of the many particle system is, that it follows stable paths were possible. Examples of stable paths are plotted in figure (9), and we therefor define the notion of stable paths rigorously as follows.

Definition 1 (stable path). *A stable path is a continuous function $x : I \to \Lambda$, which maps a time interval I into the space Λ of possible states. Furtheron there must hold for all $t \in I$*

(i) the state $x(t)$ is local minimum of $A(\cdot, t)$.

(ii) there exists an $\varepsilon > 0$ so that for all $(x_*, t_*) \in \Lambda \times I$ with $x_* \neq x(t_*)$ and $\|(x_*, t_*) - (x(t), t)\| \leq \varepsilon$, x_* is not local minimum of $A(\cdot, t_*)$.

A stable path is therefor an isolated continuous line of equilibria in Λ
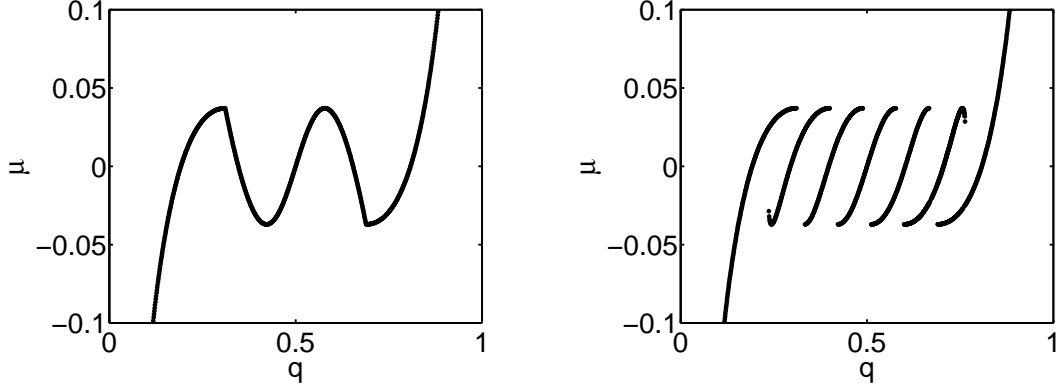

Figure 9: Stable paths of 2 and 6-particle system

This definition is rather abstract. We will now deduce further statements for the behaviour of the N-particle system by exploiting the assumption, that no particle will ever be in the intermediate region, and thus restricting Λ.

First note, that for some fixed $q < y_{**}$, as well as for $q > y^{**}$, there exists only one stable state and this case is therefore not interesting. From now on we will discuss the behaviour of the system in time intervals I where $q(t) \in (y_{**}, y^{**})$, for all $t \in I$.

Each stable path which we consider for our systems, has to belong to a fixed fraction $\lambda = k/N$, where k is the number of particles in the β-phase. This is a simple conclusion from the continuity condition for stable paths.

Lemma 2 (uniqueness and existence for stable paths with seperated phases). *For $\lambda \in [0, 1]$ fixed and any time interval I so that for all $t \in I$ there holds $q(t) \in \tilde{I}(\lambda) = (q_-(\lambda), q_-(\lambda))$, with*

$$q_-(\lambda) = \lambda y^* + (1 - \lambda)y_{**} \qquad\qquad q_+(\lambda) = \lambda y^{**} + (1 - \lambda)y_* , \qquad (55)$$

there is an uniquely (under permutations of the particles) defined stable path of the system. Furthermore the system state $x(t) = x(q(t)) = (y_1(q), y_2(q), \cdots)$ depends only on q. There exist functions $y_\lambda^-(q), y_\lambda^+(q), \mu_\lambda(q)$, which are defined on $\tilde{I}(\lambda)$, and there holds

$$q_-(\lambda) = \lambda y^* + (1 - \lambda)y_{**} \qquad\qquad q_+(\lambda) = \lambda y^{**} + (1 - \lambda)y_* \qquad (56)$$

$$y_i(q) = \begin{cases} y_\lambda^+(q) & \text{if } i \leq N\lambda = k \\ y_\lambda^-(q) & \text{else} \end{cases} \qquad (57)$$

$$\tag{58}$$

The following identities are true:

$$q = \lambda y_\lambda^+(q) + (1 - \lambda)y_\lambda^-(q) \qquad\qquad \forall q \in \tilde{I}_\lambda \qquad\qquad (59)$$

$$\mu_\lambda(q) = F'(y_\lambda^+(q)) = F'(y_\lambda^-(q)) \qquad\qquad \forall i \qquad\qquad (60)$$

$$y_\lambda^-(q_-(\lambda)) = y_{**} \qquad\qquad y_\lambda^+(q_-(\lambda)) = y^* \qquad\qquad (61)$$

$$y_\lambda^-(q_+(\lambda)) = y_* \qquad\qquad y_\lambda^+(q_+(\lambda)) = y^{**} \qquad\qquad (62)$$

Proof. It sufficises to show the existence and uniqueness of functions $y_\lambda^-(q), y_\lambda^+(q), \mu_\lambda(q)$ which fulfil (59)-(62), and to show that they are continuous.

(i) Discussion of special cases: $\lambda \in \{0; 1\}$. Here one immediately sees that

$$\lambda = 0 : \qquad I_0 = (y_{**}, y_*) \qquad y_0^-(q) = q \qquad \mu_0(q) = F'(q) , \qquad (63)$$

$$\lambda = 1 : \qquad I_1 = (y^*, y^{**}) \qquad y_1^+(q) = q \qquad \mu_1(q) = F'(q) . \qquad (64)$$

(ii) For $\lambda \in (0, 1)$ we first construct the function μ_λ. Therefore we define the function

$$g_0|_{[\mu_*, \mu^*]} := \left(\mu^0|_{[y_*, y_{**}]}\right)^{-1} \qquad g_1|_{[\mu_*, \mu^*]} := \left(\mu^1|_{[y^{**}, y^*]}\right)^{-1} \qquad (65)$$

$$g_\lambda|_{[\mu_*, \mu^*]} := \lambda g_1 + (1 - \lambda)g_0. \qquad (66)$$

For $q \in \tilde{I}(\lambda)$ there must hold for μ_λ as defined

$$g_\lambda(\mu_\lambda(q)) = q. \qquad (67)$$

Recall the condition of the model: $0 \leq \mu_1', \mu_2' \leq c_0$ and therefor

$$g_0' \geq c_1 := \frac{1}{c_0} \qquad g_1' \geq c_1 > 0 \qquad (68)$$

$$\Rightarrow g_\lambda' \geq c_1 \qquad \tilde{I}_\lambda = (\lambda y^* + (1 - \lambda)y_{**}, \lambda y^{**} + (1 - \lambda)y_*) \qquad (69)$$

$$\Rightarrow \mu_\lambda|_{I_\lambda} := \left(g_\lambda|_{[\mu_*, \mu^*]}\right)^{-1} \qquad \text{exists uniquely and is continuous, and} \qquad (70)$$

$$0 \leq \mu_\lambda'|_{I_\lambda} \leq c_0 . \qquad (71)$$

Now we define y_λ^-, y_λ^+ as the continuous functions

$$y_\lambda^-(q) := \mu_0^{-1}(\mu_\lambda(q)) = g_0(\mu_\lambda(q)) \qquad y_\lambda^+ := \mu_1^{-1}(\mu_\lambda(q)) = g_1(\mu_\lambda(q)) , \qquad (72)$$

which are defined on $\tilde{I}_\lambda$. Note that (59)-(62) is true by construction.

Since this is (under permutations) the only stable path for the system, for fixed λ, there are no local minima near by. The positive definiteness of the second derivative is trivially given by the condition that all particles are in stable states. $\qquad\square$

Note that hereby the three system describing values μ, q, λ are dependent of each other. If two of them are given, the third value is uniquely determined. That means that by knowing two of those system values one knows the whole system state (with respect to permutations).

We want to show, that the distance of two potential curves $\mu_\lambda(q), \mu_{\lambda+\delta}(q)$ vanishes if $\delta \to 0$. This assertion requires a definition of the distance. Note that by construction of μ_λ a horizontal line between μ_λ and $\mu_{\lambda+\delta}$ at an arbitrary height $\mu_\lambda(q_1) = \mu_{\lambda+\delta}(q_2)$ has the length δ.

This might already prove the assertion, but we consider another notation of distance.

Definition 2 (vertical distance between two potential curves). *We define the vertical distance of two potential curves μ_λ and $\mu_{\lambda+\delta}$ ($\delta > 0$) at a certain point $q \in \tilde{I}_\lambda \cup \tilde{I}_{\lambda+\delta}$ as*

$$
d(\mu_\lambda, \mu_{\lambda+\delta}, q) = \begin{cases} \mu_\lambda(q) - \mu_{\lambda+\delta}(q) & q \in \tilde{I}_\lambda \cap \tilde{I}_{\lambda+\delta} \\ \mu^* - \mu_* & \text{if } \tilde{I}_\lambda \cap \tilde{I}_{\lambda+\delta} = \emptyset \\ \mu_\lambda(q) - \mu_* & \text{if } q \in \tilde{I}_\lambda \backslash \tilde{I}_{\lambda+\delta} \text{ and } \tilde{I}_\lambda \cap \tilde{I}_{\lambda+\delta} \neq \emptyset \\ \mu^* - \mu_{\lambda+\delta}(q) & \text{if } q \in \tilde{I}_{\lambda+\delta} \backslash \tilde{I}_\lambda \text{ and } \tilde{I}_\lambda \cap \tilde{I}_{\lambda+\delta} \neq \emptyset \end{cases} , \tag{73}
$$

as well as the total vertical distance of two potential curves as

$$
d(\mu_\lambda, \mu_{\lambda+\delta}) = \max_{q \in \tilde{I}_\lambda} d(\mu_\lambda, \mu_{\lambda+\delta}, q) . \tag{74}
$$

Note that for $\tilde{I}_\lambda \cap \tilde{I}_{\lambda+\delta} \neq \emptyset$ there holds

$$
\max_{q \in I_\lambda \cap I_{\lambda+\delta}} d(\mu_\lambda, \mu_{\lambda+\delta}, q) \geq \max_{q \in I_\lambda \backslash I_{\lambda+\delta}} d(\mu_\lambda, \mu_{\lambda+\delta}, q) . \tag{75}
$$

4.3 Dynamic behaviour

So far we have been able to describe the behaviour of the system as long as it stays on the above described stable paths. Crucial was the assumption, that the macroscopic quantity $q(t)$ has to stay for the considered times in an open set $\tilde{I}_\lambda$.

The question we are addressing in this subsection, is what happens if the macroscopic state $q(t)$ runs over the boundary of $\tilde{I}_\lambda$. For simplicity we only discuss the case were $q(t)$ is increasing in time and runs over the top boundary $q^+(\lambda) = q(t_*)$ at a certain time t_*. By assuming a continuous (in time) system state $x(t)$, one can uniquely determine the state $x(t_*)$. The positive definiteness of the second derivate and therefore the equilibria demand is not guaranteed at this limit state. However for $q(t) > q^+(\lambda)$ there is no equilibria point of the energy which suffices the condition of the particle fraction λ in α-phase and β-phase. Thus we call this state a critical point.

We describe the system state evolution for $q(t)$ moving increasingly over $q^+(\lambda)$ by a model assumption. We say that the system state changes discontinuously. One particle which was in the α-phase changes to the β-phase and therefore the system describing fraction $\lambda(t)$ changes: $\lambda(t_* + \varepsilon) = \lambda(t_*) + 1/N$ for ε small enough.

In the plot of the stable paths this means, that the systems potential is described by μ_λ and the potential drops to the potential curve $\mu_{\lambda+\frac{1}{N}}$ as q increases over the

critical point. Note that for N large enough there holds for all $\lambda = k/N \in [0, 1]$ that $q^+(\lambda) \in \tilde{I}_\lambda \cap \tilde{I}_{\lambda + \frac{1}{N}}$ and so the above described behaviour is possible.

To describe the resulting dynamic behaviour of the constructed model we give evolutionary laws for the state parameter $\lambda(t)$ in dependence of smooth functions $q(t), \dot{q}(t), t \in I = [t_0, t_1]$ and a state $\lambda(t_0)$ at a starting time t_0.

(i) Prerequisite of allowed starting state: $0 \le \lambda(0) = K/N \le 1$ is a fraction and $q(0) \in \overline{\tilde{I}_{\lambda(0)}}$.

(ii) For $q(t) \in \tilde{I}_{\lambda(t)}$ or $\dot{q}(t) = 0$, the fraction $\lambda(t)$ stays unchanged/constant.

(iii) $\lambda < 1, q(t_*) = q^+(\lambda)$ and $\dot{q}(t_*) > 0$, then λ increases by $1/N$ at time t_* That means that there exists an $\varepsilon > 0$ so that for all $t > t_*, |t - t_*| < \varepsilon$ there holds $\lambda(t) = \lambda(t_*) + 1/N$.

(iv) $\lambda > 0, q(t_*) = q^-(\lambda)$ and $\dot{q}(t_*) < 0$, then λ decreases by $1/N$ at time t_* That means that there exists an $\varepsilon > 0$ so that for all $t > t_*, |t - t_*| < \varepsilon$ there holds $\lambda(t) = \lambda(t_*) - 1/N$.

This way there is at all times a fraction λ defined and the system state $x(t)$ can be determined by $q(t)$ and $\lambda(t)$. Looking at the macroscopic observable quantities q and $\mu_\lambda(q)$, one observes an hysteretic behaviour as seen in figure (10).
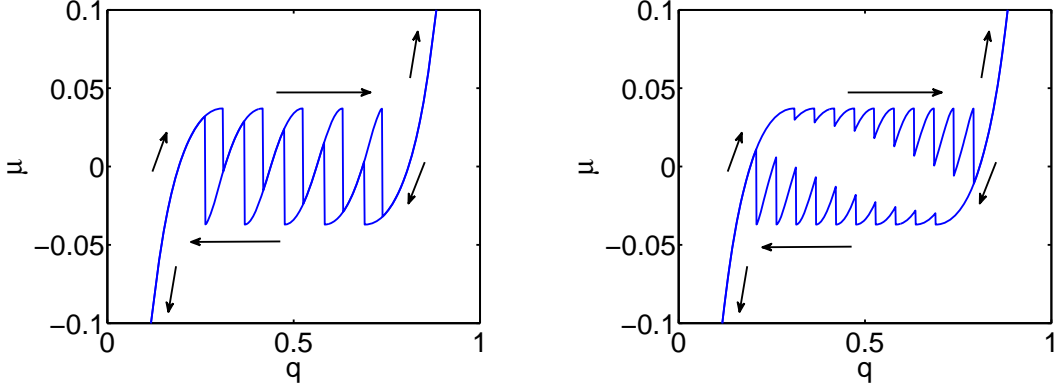

Figure 10: Hysterese of 5 and 10-particle system

.

Lemma 3 (vertical distance vanishes)**.** *For an arbitrary $\varepsilon > 0$ there exists a $\delta_* > 0$, so that for all $0 < \delta < \delta_*$ and $\lambda \in [0, 1]$ there holds*

$$d(\mu_\lambda, \mu_{\lambda + \delta}) \le \varepsilon . \tag{76}$$

Proof. First assume, that δ_* is small enough, so that for all $0 < \delta \le \delta_*$ we can guarantee $I_\lambda \cap I_{\lambda + \delta} \ne \emptyset$. It suffices to bound the distance for $q \in I_\lambda \cap I_{\lambda + \delta}$ is

24

bounded.

$$0 \leq d(\mu_\lambda, \mu_{\lambda+\delta}, q) = \mu_\lambda(q) - \mu_{\lambda+\delta}(q) \tag{77}$$

$$= \underbrace{\mu_\lambda(q) - \mu_{\lambda+\delta}(q+\delta)}_{=0 \text{ by constr.}} + \int_q^{q+\delta} \mu'_{\lambda+\delta}(s)\mathrm{d}s \tag{78}$$

$$\leq c_0\delta \qquad \text{due to (71)} . \tag{79}$$

$\square$

The maximal vertical distance between two neighbouring potential curves vanishes as N increases.

4.4   Asymptotic behaviour and hysterese

The evolutionary description of our model in the last section looks similar to an ordinary differential equation. One could interpret the jumping of the internal state variable λ as a derivative being a delta distribution.

In this case one can formally deduce an asymptotic evolution law for particle number $N \to \infty$. We call this the macroscopic model.

(i) Prerequisite of allowed starting state: $\lambda(0) \in [0,1]$ and $q(0) \in \overline{\tilde{I}_{\lambda(0)}}$.

(ii)

$$\dot\lambda = \begin{cases} 0 & q(t) \in I_{\lambda(t)} \text{ or } \dot{q}(t) = 0 \\ \dot{q}(t) & q = q^+(\lambda), \dot{q}(t) > 0 \text{ and } \lambda < 1 \\ \dot{q}(t) & q = q^-(\lambda), \dot{q}(t) < 0 \text{ and } \lambda > 0 \end{cases} \tag{80}$$

We will now show that the observable behaviour of the potential for the N-particle system, denoted $\mu_N(t)$, converges uniformly to the behaviour of the macroscopic model $\mu(t)$. This can be observed in figure (11).

Lemma 4 (convergence of potentials as for large particle numbers). *Let $q(t) \in C^2([t_0, t_1])$ be a given evolution of the macroscopic system state, and let $\lambda_0 \in \mathbb{Q} \cap [0,1]$ be an allowed starting value for the internal state of the macroscopic model. Then for a series of numbers $N_\ell, \ell = 1, 2, \ldots$ and $N_\ell > N_{\ell+1}$ so that the rational value $\lambda_0 = K_\ell/N_\ell$ can be represented as a fraction with denominator N_ℓ there holds the following.*

For $\lambda_\ell(t)$ being the evolution for the internal system state of the N_ℓ-particle system and $\lambda(t)$ the evolution of the macroscopic model respectively, we have uniformly convergence of the potentials, i.e. for all $\delta > 0$ there exists a $N_\star > 0$ s.t.

$$\max_{[t_0,t_1]} |\mu_{\lambda_\ell(t)}(q(t)) - \mu_{\lambda(t)}(q(t))| \leq \delta \qquad\qquad \forall N \geq N_\star. \tag{81}$$
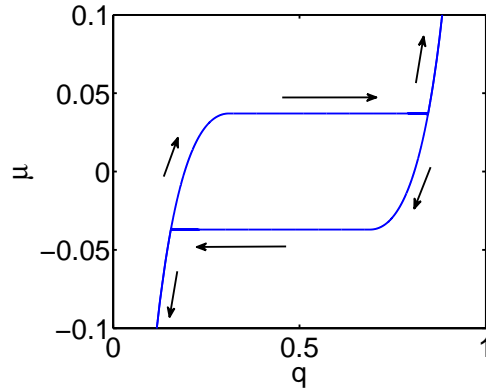
25

Figure 11: Hysterese 1000-particle system

Proof. First one should notice, since the macroscopic model as well as the N_ℓ-particle model start from the same state $q(t_0), \lambda(t_0)$ the difference $|\lambda(t) - \lambda_\ell(t)| \leq 1/N_\ell$ and therefor the assertion is proved by the former lemma for the vanishing vertical distance. $\square$

Path-Dependence. In a lithium battery it is observable that the voltage for the same charge state depend on the battery history [18]. This path- dependence can be explained with our model. We want to reproduce the following experiment which is described in short:

- process starts with an empty battery $(q = 1)$

- battery will be half charged $(q = 0.5)$

- then fully charge of the battery $(q = 0)$

- after this discharge to half charge state $(q = 0.5)$

- at last again fully charged $(q = 0)$

In the experiment the battery undergoes a loading process $q(t) : [t_0, t_1] \to [0, 1]$. The same loading process is done twice, but different behaviour is observed. The only difference is, that the same state $q(t_0) = .5$ where the loading starts is reached through different paths. Either by loading from an 'empty' state of the battery or by unloading from a 'full' state.

The simulation 12 shows an evolution of the potential for the described experiment. One observes that the voltage from the second loading process is lower than in the first case. This is due to different internal states $\lambda(t)$ even though the system has the same loading state $q(t)$.

Mechanical dependence. In the argumentation before, the pressure p_E (cf. (29)) was constant. On the otherhand taking the change of volume of the particles into
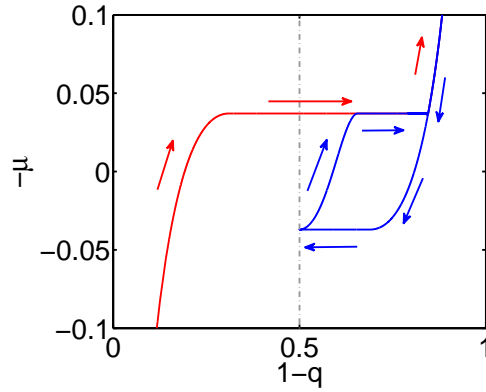
Figure 12: Path-dependence,1000 particle

account, one can model an arising stress in the electrolyte as q increases. This means p_E is a function of q and enters into the pressure term of the chemical potential (16). With this model we can reproduce a slope of the plateau in the system's potential curves. The simulation 13 shows such an influence in an exaggerated way for the lithium model. This should be incorporated in the model of hydrogen storage as well, where slopes of plateaus have been observed in experiments, and are steeper than in the Lithium case. The explanation could be the big volumechange during loading of possible up to 30 % of the magnesia.
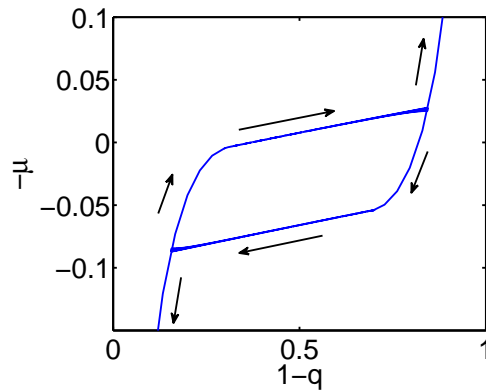

Figure 13: Mechanical interaction of the particles, 250 particle

5 An illustrative analogy: Inflation of connected rubber balloons

We consider N connected spherical rubber balloons indexed by $l \in 1, 2, ..., N$ as it is indicated in Figure 14. Via the pressure vessel the balloons can be simultaneously

inflated with air.

The pressure difference $p^l - p_0$ of each balloon with respect to the outer pressure p_0, is related to its radius

$$p^l - p_0 = \alpha \left(\frac{R}{r^l} - \left(\frac{R}{r^l} \right)^7 \right) \left(1 + \beta \left(\frac{r^l}{R} \right)^2 \right), \tag{82}$$

where R is the radius of the undeformed balloon and α and β are related to the initial thickness of the balloon and to the elastic constants of rubber, more details are found in [5] and [14].

The function (82) is a non-monotone function, which induces qualitatively the same behaviour as the chemical potentials of the study from above.
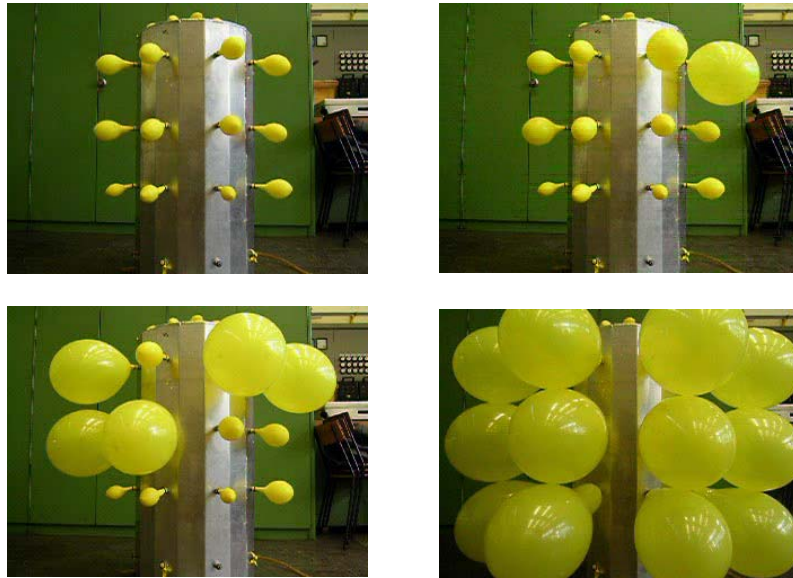

Figure 14: Four different states of connected rubber balloons during loading with air via the pressure vessel.

In case that a single balloon is inflated by supply of air under fixed pressure, the decreasing part of the pressure-radius relation is an unstable branch. However, it can be shown, that if a balloon with a fixed filling grows due to a decrease of the outer pressure, that branch is stable.

Now we consider the process that is illustrated by Figure 14. There is a constant supply of air into the pressure vessel and that air freely distributes among the balloons. The following happens: As long as the filling of balloons are small, they all have the same size until they reach with increasing filling the end of the first increasing pressure-radius branch. Careful observation now reveals that only one balloon will pass quickly through the decreasing branch to an apparent larger radius, whereas the other balloons slightly decrease at first their radius before all balloons increase their radius due to the constant supply of air. In this time regime we thus

have one large balloon and $N - 1$ small ones. This regimes ends when the small balloons again reach the end of the first increasing pressure-radius branch, and here the same event as before happens. One balloon passes to a larger radius, whereas now $N - 2$ balloons fall back, and we have now a state with 2 large balloons and $N - 2$ small ones. This process is repeated until all balloon have the same large size. Last state of the sequence from figure 14.

The interpretation and in particular the analogy to the behaviour of many particles in the two storage problems from above is obvious. There is a regime of two coexisting phases, formed by small respectively large balloons. Each balloon is a homogeneous and single phase object, however, some balloons are in one phase and the others are in the other phase. See [9], [10] and [14] for more details.

Acknowledgments

References

[1] Von B. Bogdanović, *Katalytische Synthese von Organolithium- und -magnesium- Verbindungen sowie von Lithium- und Magnesiumhydriden - Anwendungen in der organischen Synthese und als Wasserstoffspeicher*, Angew. Chem. 97 (1985) 253-264

[2] W. Dreyer and F. Duderstadt, *On the modelling of semi-insulating GaAs including surface tension and bulk stresses*, WIAS Preprint No. 995, to appear in Proc. R. Soc. A (2008).

[3] W. Dreyer, M. Gaberšček and J. Jamnik, *Phase transition and hysteresis in a rechargeable lithium battery*, WIAS Preprint No. 1284 (2007)

[4] W. Dreyer, C. Guhlke and R. Huth, *Sharp interface modelling and simulations of hydrogen storage in crystals*, in preparation

[5] W. Dreyer, I. Müller and P. Strehlow, *A study of equilibria of interconnected balloons*, Quarterly J. Mech. Appl. **35** (1982), p. 419.

[6] J.M. Ell, *Gasinduziertes optisches Schaltverhalten dünner Magnesium-Nickel-Schichten*, Dissertation, TU Darmstadt, Fachbereich Material- und Geowissenschaften (2007)

[7] B.C. Han, A. Van der Ven, D. Morgan and G. Ceder, *Electrochemical modeling of intercalation processe with phase field models*, Electrochimica Acta **49** (2004), 4691–4699.

[8] W. Klose and V. Stuke, *Untersuchung zur Wasserstoff-Speicherung im System Magnsium/Magnesiumhydrid*, Chem.-Ing.-Tech. 64 (1992) Nr. 4, S. 360-361

[9] W. Kitsche, *Modellierung eines Phasenüberganges an einem System vieler Ballons*, Diploma thesis, TU Berlin (1985).

[10] W. Kitsche, I. Müller and P. Strehlow, *Simulation of pseudoelastic behavior in a system of rubber balloons*, In: Metastability and incompletely Posed Problems, IMA Vol. **3** (2004), p. 2113.

[11] T. Maxisch and G. Ceder, *Elastic properties of olivine Li_xFePO_4 from first principles*, Physical Reviev B**73** (2006), 174112-1–174112-4.

[12] A. Mielke and L. Truskinovsky *Pseudoelasticity as limit of a bistable chain with small viscosity*, Workshop, Phase Transitions and Optimal Control WIAS Berlin, 23. - 25. October 2008

[13] I. Müller, *Thermodynamics, Interaction of Mechanics and Mathematics Series*, Pitman Advanced Publishing Program, Boston, 1985.

[14] I. Müller and P. Strehlow, *Rubber and Rubber Balloons*, Lecture Notes in Physics **637**, Springer (2004).

[15] T. Nietsch, T. Domschke, A. Rickert and E. Schütt, *Messung und Berechnung der Gleichgewichtsisothermen für Wasserstoff in einem Metallhydrid bei Beladungsgraden kleiner 0,2%*, Chem.-Ing.-Tech. 64 (1992) Nr. 11, S. 1024-1026

[16] G. Puglisia and L. Truskinovsky, *Rate independent hysteresis in a bi-stable chain*, Journal of the Mechanics and Physics of Solids 50 (2002) 165 âĂŞ 187

[17] V. Srinivasan and J. Newman, *Discharge Model for the Lithium Iron-Phosphate Electrode*, Journal of The Electrochemical Society **151**(10) (2004), A1517–A1529.

[18] V. Srinivasan and J. Newman, *Existence of Path-dependence in the LiFePO4 Electrode*, Electrochemical and Solid State Letters, 9, A110 (2006)

[19] M. Wagemaker, W.J.H. Borghols and F.M. Mulder, *Large Impact of Particle Size on Insertion Reaction. A Case for Anatase Li_xTiO_2*, J. AM. CHEM. SOC. **129**(14) (2007), 4323–4327.

[20] A. Yamada, H. Koizumi, S.I. Nishimura, N. Sonoyama, R. Kanno, M. Yonemura, T. Nakamura and Y. Kobayashi, *Room-temperature miscibility gap in Li_xFePO_4*, Nature materials Letters **5** (2006), 357–360.